Contents lists available at ScienceDirect

Pharmacological Research

journal homepage: http://ees.elsevier.com

Fatty acid sensing GPCR (GPR84) signaling safeguards cartilage homeostasis and protects against osteoarthritis

Fanhua Wang [a,1], Lu Ma [a,1], Yi Ding [a,1], Liang He [a], Mingzhi Chang [a], Yingquan Shan [a], Stefan Siwko [b], Geng Chen [a], Yuwei Liu [a], Yunyun Jin [a,*], Xiaochun Peng [c,**], Jian Luo [a,*]

[a] Shanghai Key Laboratory of Regulatory Biology, Institute of Biomedical Sciences and School of Life Sciences, East China Normal University, Shanghai, 200241, PR China
[b] Institute of Biosciences and Technology, Texas A&M University Health Science Center, Houston, TX, 77030, USA
[c] Department of Orthopaedics, The Sixth Affiliated People's Hospital, Shanghai Jiaotong University, Shanghai, 200233, PR China

ARTICLE INFO

Chemical compounds studied in this article
IL-1β (PubChem CID: 123872)
Lauric acid (PubChem CID: 3893)
6-OAU (PubChem CID: 10354234)

Keywords
Fatty acid
GPR84
Osteoarthritis
Cartilage
ECM
Cartilage anabolism and catabolism

ABSTRACT

It is well known that free fatty acids (FFAs) have beneficial effects on the skeletal system, however, which fatty acid sensing GPCR(s) and how the GPCR(s) regulating cartilage development and osteoarthritis (OA) pathogenesis is largely unknown. In this study, we found Gpr84, a receptor for medium-chain FFAs (MCFA), was the only FFA-sensing GPCR in human and mouse chondrocytes that exhibited elevated expression when stimulated by interleukin (IL)-1β. *Gpr84*-deficiency upregulated cartilage catabolic regulator expression and downregulated anabolic factor expression in the IL-1β-induced cell model and the destabilization of the medial meniscus (DMM)-induced OA mouse model. *Gpr84*$^{-/-}$ mice exhibited an aggravated OA phenotype characterized by severe cartilage degradation, osteophyte formation and subchondral bone sclerosis. Moreover, activating Gpr84 directly enhanced cartilage extracellular matrix (ECM) generation while knockout of Gpr84 suppressed ECM-related gene expression. Especially, the agonists of GPR84 protected human OA cartilage explants against degeneration by inducing cartilage anabolic factor expression. At the molecular level, GPR84 activation inhibited IL-1β-induced NF-κB signaling pathway. Furthermore, deletion of *Gpr84* had little effect on articular and spine cartilaginous tissues during skeletal growth. Together, all of our results demonstrated that fatty acid sensing GPCR (Gpr84) signaling played a critical role in OA pathogenesis, and activation of GPR84 or MCFA supplementation has potential in preventing the pathogenesis and progression of OA without severe cartilaginous side effect.

1. Introduction

Osteoarthritis (OA), the most common degenerative joint disease and a major cause of pain and disability in adults, incurs an enormous economic burden on society [1,2]. Although OA was primarily thought to be driven only by cartilage degradation, but more recently other pathological processes including osteophyte formation, subchondral bone sclerosis and synovial inflammation were found to contribute to OA [3–5]. Numerous etiologic risk factors for the development of OA such as mechanical stress, aging, obesity and metabolic syndrome were identified through preclinical research in animal models of OA and clinical studies in patients with OA [6–9]. However, the molecular mechanisms regulating these processes in articular chondrocytes remain unclear. It has been established that nuclear factor-κB (NF-κB) and mitogen-activated protein kinases (MAPKs) signaling orchestrates mechanical, inflammatory, oxidative stress activated processes and

Abbreviations: ACAN, Aggrecan; Adamts5, a disintegrin and metalloproteinase with thrombospondin motifs; ANOVA, One way analysis of variation; BMD, bone mineral density; BV/TV, bone volume per tissue volume; cDNA, Complementary DNA; Col2a1, collagen type II alpha 1 chain; Col10a1, collagen type X alpha 1 chain; DMM, destabilization of the medial meniscus; ECM, extracellular matrix; FBS, fetal bovine serum; FFA, free fatty acid; GADPH, Glyceraldehyde 3-phosphate dehydrogenase; GPCR, G protein–coupled receptor; GZ, growth plate zone; H&E, hematoxylin and eosin; HZ, hypertrophic zones; IHC, immunohistochemistry; IL-1, interleukin 1; IL-1β, interleukin 1 beta; IL-6, interleukin 6; MAPK, mitogen-activated protein kinase; Mmp3, matrix metalloproteinase 3; Mmp12, matrix metalloproteinase 12; Mmp13, matrix metalloproteinase 13; MCFA, medium-chain fatty acid; MFC, medial femoral condyle; MTP, medial tibial plateau; NF-κB, nuclear factor-κB; OA, osteoarthritis; OARSI, Osteoarthritis Research Society International; OSM, oncostatin M; Prg4, proteoglycan 4; PZ, proliferating zone; P1, Postnatal day 1; RZ, resting zone; RNAi, RNA interfere; RT-qPCR, real-time quantitative PCR; SBP, subchondral bone plate; siRNA, small interfering RNA; Sox9, SRY-box; S.D, standard deviation; Tb.N, trabecular number; Tb.Th, trabecular thickness; Tb.Sp, trabecular spacing; TV, total tissue volume; WT, wild-type; 6-OAU, 6-*n*-octylaminouracil.

* Corresponding authors at: Shanghai Key Laboratory of Regulatory Biology, The Institute of Biomedical Sciences, School of Life Sciences, East China Normal University, 500 Dongchuan Road, Shanghai, 200241, PR China.
** Corresponding authors at: Department of Orthopaedics, The Sixth Affiliated People's Hospital, Shanghai Jiaotong University, 600 Yishan Road, Shanghai, 200233, PR China.
E-mail addresses: yyjin@bio.ecnu.edu.cn (Y. Jin); dr.xcpeng@foxmail.com (X. Peng); jluo@bio.ecnu.edu.cn (J. Luo)
[1] These authors contributed equally to this manuscript

https://doi.org/10.1016/j.phrs.2020.105406
Received 4 October 2020; Received in revised form 28 November 2020; Accepted 18 December 2020
Available online xxx
1043-6618/

ECM degradation that contribute to cartilage tissue damage [10–12]. Whereas, few effective pharmacologic or other therapies for OA have been developed.

It has been reported that free fatty acids (FFAs) contributes to the skeletal health, as increasing the supplementation of long-chain ω-3 fatty acids positively contribute to joint health and preventing osteoporosis [13–16]. Short-chain fatty acids augment systemic bone mass by protecting from bone resorption [17,18] and suppress inflammation in chondrocytes [19]. However, few studies have investigated medium-chain fatty acids' (MCFAs) effect on the skeletal system, particularly on joint health.

Recent studies showed that FFAs bind several types of membrane receptors, to activate multiple intracellular signal transduction pathways. Five G protein–coupled receptors, GPR40, GPR41, GPR43, GPR84 and GPR120, have been reported to be activated by FFAs, in which GPR40 and GPR120 are receptors for long-chain fatty acids, GPR41 and GPR43 for short-chain fatty acids, while GPR84 for MCFAs [20]. Studies showed that these FFA-sensing GPCRs have important physiological significance in maintaining glucose stability, adipose formation, immune function, energy metabolism and other physiological processes [21–26]. The regulatory roles of the FFA-sensing GPCRs in the pathogenesis and progression of OA still need to be further investigated. In recent years, some studies suggested a direct relationship between FFA-sensing GPCRs and OA. Manifestations of knee joint instability-induced OA were aggravated in *Gpr40*$^{-/-}$ mice, and *Gpr40*$^{-/-}$ chondrocytes secreted more inflammatory mediators and showed decreased anabolism upon IL-1β treatment [27]. *Gpr120*$^{-/-}$ mice displayed an accelerated development of anterior cruciate ligament transection surgery-induced OA, including modest inflammation, cartilage degeneration, and aberrant changes in subchondral bone [28]. However, current understanding is limited regarding whether other FFA-sensing GPCRs participate in the pathogenesis and progression of OA and how they could manipulate signal transduction.

GPR84 was identified as a receptor for MCFAs, and is specifically activated by C9-C12 saturated fatty acids. MCFAs derived from milk of certain species and coconut oil have a role in bone mass and bone remodeling [29,30]. Previous studies showed that GPR84 was expressed on immune cells mediating proinflammatory and immunostimulatory effects [31–33]. Moreover, GPR84 was associated with obesity and diabetes, participating in lipid metabolism [24]. Recently, GPR84 was also reported to be highly abundant in skeletal muscle, where it played a critical role in the regulation of mitochondrial integrity [30]. Preliminary *in vitro* evidence indicates that GPR84 has a role in osteoclastogenesis [34]. However, the role of GPR84 function in cartilage biology is poorly investigated to date.

In this study, we found the MCFAs receptor Gpr84 was the only FFA-sensing GPCR in human and mouse chondrocytes that exhibited increased expression when stimulated by IL-1β. *Gpr84*-deficiency aggravated OA pathogenesis *in vitro* and *in vivo*. Moreover, Gpr84 affected articular cartilage homeostasis *via* altering extracellular matrix production and degradation. Activating GPR84 could protected human OA cartilage explants from degeneration through enhancing cartilage anabolic factor expression. Furthermore, loss of *Gpr84* had little effect on articular and spine cartilaginous tissues during physiological skeletal growth. Overall, our data demonstrated the importance of the FFA-sensing GPCR, Gpr84, in maintaining cartilage homeostasis and provides a novel target for potential therapeutic interventions in the treatment of osteoarthritis.

2. Materials and methods

2.1. Mice

Ggr84 knockout mice were generated using the CRISPR/Cas9 system in the C57BL/6 J mouse strain, and Ggr84$^{-/-}$ generation was performed by the Animal Center of East China Normal University. Ggr84$^{-/-}$ mice were missing 172bp and identified by PCR using tail DNA. Primers for the knockout mice genotyping are listed in Table 1. Maintenance, use and treatment of all animals was in accordance with accepted standards of the Ethics Committee at East China Normal University. All mice were housed in groups of five. Pathogen-free barrier facilities were used for all animals. A 12 -h light/dark cycle was maintained at all times. The mice were monitored daily and the weights were monitored weekly throughout the experiment to ensure health status. No adverse events were observed during the experiments. Except for the animal experiment with DMM surgery, Ggr84$^{-/-}$ and WT littermates were allocated into groups based on sex, age, and genotype. After the selection, mice were allocated randomly without subjective judgement. The numbers of mice per group were indicated in the figure legends. To reduce animal use, we analyzed multiple organs in the same mice including articular cartilage, growth plate of long bone and cartilaginous tissue of spine.

2.2. Experimental OA in mice

Experimental OA was induced by destabilization of the medial meniscus (DMM) surgery in 8-week-old male mice; In brief, mice were anesthetized and then the joint capsule of right knee medial to the patellar tendon was excised. The medial meniscotibial ligaments were cut with microsurgical bistoury. Sham operation mice with only medial capsulotomy were used as controls [35]. Mice were killed 8 weeks after the DMM surgery, and samples of the knee joints were fixed in 4% paraformaldehyde and then processed for micro-CT and histological analysis.

2.3. Micro-CT analyses

Samples of the knee joints fixed in 4% paraformaldehyde were washed with PBS and scanned using x-ray microtomography (SKYSCAN 1272, Bruker microCT). The scanner was set at a voltage of 60.0 kVp, a current of 166.0 μA and a resolution of 7.0 μm per pixel. Next, we defined the region of interest as ROI to cover the subchondral bone medial compartment. Three-dimensional structural measurements of the ROI were analyzed to determine the total tissue volume (TV) of subchondral bone. Five consecutive images from the medial tibial plateau were performed for three-dimensional reconstruction. For tibia trabeculae bone samples were scanned at a tube potential of 60.0 kV, 166.0 μA and a resolution of 9.0 μm pixels. The tibia sample area selected for measurement was 0.7 mm below the growth plate. Trabecular bone pa-

Table 1
Identification of knockout mice.

Genotype primer	Result judgement	PCR process
F:AGGCCTGAGAATCTTTGTGAGCTA	WT: 782 bp	95 °C, 5 min;
R:GCCGGTACGCCAATGGAG	*Ggr84* $^{-/-}$: 610 bp	95 °C, 30 s; 60 °C, 30 s; 72 °C, 40 s; 35 cycles 72 °C, 5 min; 25 °C, hold. Polymerase: Taq DNA polymerase

*F = Forward Primer, *R = Reverse Primer.

rameters of the tibia were calculated using CTan software (Bruker microCT). Three-dimensional reconstruction images were produced with CTVOL (Bruker microCT).

2.4. Histological analyses

Following micro-CT analysis, the knee joints were decalcified with 0.5 M EDTA for 3 weeks and embedded in paraffin. The knee joint was cut in serial sections of 6 μm thickness and sections were deparaffinized in xylene, hydrated with graded ethanol and stained with Safranin-O and H&E. An OARSI scoring system was used in evaluating articular destruction including medial tibial plateau, medial femoral condyle and sum scoring by blinded observers [35]. Synovitis was evaluated according to a previously described scoring system [36]. Osteophyte maturity was quantified as previously described [35]. The thickness of the subchondral bone plate was measured as previously described [37]. The articular cartilage, growth plate and cartilage tissues of the spine histomorphometric measurements were performed *via* microphotographed sections. For immunohistochemical staining, mouse joint sections were deparaffinized, hydrated and treated with 20 μg/mL Proteinase K for 20 min followed by 3 % H_2O_2 for 10 min. Then, sections were incubated overnight at 4 ˚C with antibodies followed by ABC Kit reagents (Vector Laboratories, Burlingame, CA, USA). Signals were visualized with the DAB Substrate Kit followed by counterstaining with Harris' hematoxylin. For immunofluorescent staining, secondary antibodies conjugated with fluorescence were added, and sections were incubated for 1 h at room temperature without light. Primary antibodies for immunohistochemical and immunofluorescent staining were used: Col10a1 (1:1000; Abcam; ab58632), Mmp13 (1:100; Abcam; ab39012), Col2a1 (1:100; Abcam; ab34712) and Acan (1:100; Proteintech; 13880−1-AP). Sections were microphotographed with an Olympus microsystems microscope (Olympus Corporation, Tokyo, Japan) and analyzed using Image J software.

2.5. Pain assay

OA-associated pain in mice was measured using the von Frey assay after surgery. Mice were kept in a quiet environment and allowed to acclimate for at least 60 min. Mechanical allodynia was tested with von Frey filaments (Ugo Basile Biological Research Apparatus Company, Milan, Italy) *via* up-down methods [38]. The test was performed by individuals who were blinded to the information of the mice under analysis. The examination was repeated three times, and the mean data was calculated.

2.6. Cell culture

Primary mouse chondrocytes were isolated from new-born mouse (postnatal day 3) articular cartilage by 0.2 % collagenase type II (Gibco, Thermo Fisher Scientific, Waltham, MA, USA). Mouse articular chondrocytes were maintained in DMEM/F12 (Gibco, Thermo Fisher Scientific, Waltham, MA, USA) supplemented with 1 % penicillin/streptomycin and 10 % (v/v) fetal bovine serum (FBS). Only the passage 1–2 mouse chondrocytes were used for experiments. Normal primary human chondrocytes were purchased from BeNa Culture Collection (Beijing, China). Human chondrocytes were maintained in DMEM supplemented with 10 % FBS, 1 % L-glutamic acid, and 1 % antibiotics. Human chondrocytes were provided at passage 1, and passages 2–3 were used for experiments. ATDC5 cells were cultured in DMEM containing 10 % FBS. For western blotting assay, ATDC5 cells were treated with IL-1β (10 ng/mL) for the indicated time periods in the presence of 6-OAU (5 μM) and lauric acid (50 μM). Human chondrocytes and mouse chondrocytes were seeded at a density of 80,000 cells per well in 24-well plates and allowed to adhere overnight. Human and mouse chondrocytes were treated with IL-1β (1 ng/mL) (R&D System, Minneapolis, MN, USA) for 24 h and then used for the next experiment. For chondrogenesis assessed, the mouse articular chondrocytes were allowed to grow to 80 – 90 % confluence and then differentiated in differentiation medium for 14 days with or without 6-OAU and lauric acid. For siRNA transfection in mouse chondrocytes, siRNA (GenePharma, Shanghai, China) and Lipofectamine 2000 (Invitrogen, Carlsbad, CA, USA) were transfected in chondrocytes according to the manufacturer's instructions.

2.7. Culture of human OA cartilage explants

We obtained samples from knee joint cartilage of OA patients undergoing total knee arthroplasty, with the approval of the Human Ethics Committee of Shanghai Changhai Hospital (CHEC2020−131). OA cartilage explants were cut into pieces of approximately 2 mm^3 in volume from relatively healthy parts of femoral condyles cartilages of total knee arthroplasty patients. The explants were cultured in DMEM containing 5 % FBS supplemented with 6-OAU (5 μM) or lauric acid (50 μM) or vehicle control. After 2 weeks, cartilage explants were collected for mRNA expression levels examination.

2.8. Cell viability assay

Normal primary human chondrocytes were purchased from BeNa Culture Collection (Beijing, China). Human chondrocytes were seeded at a density of 10,000 cells per well in 96-well plates and allowed to adhere overnight. Cells were then treated with 6-OAU or lauric acid for 48 h. Cell viability was measured with a commercial CCK-8 kit (Dojindo, Japan) according to the manufacturer's instructions.

2.9. RNA assay

Total RNA was extracted from primary cultured chondrocytes using the TRIZOL reagent (Invitrogen, Carlsbad, CA). cDNA was obtained *via* PrimeScript™ RT reagent Kit (TaKaRa Bio, Kyoto, Japan) and PCR-amplified using the PCR primers. Quantitative RT-PCR was performed using the SYBR Green Master Mix (Yeasen, Shanghai, China) on the Step One Plus PCR system (AB Applied, Life Technologies, Thermo Fisher Scientific, Waltham, MA, USA). Individual target genes were normalized relative to glyceraldehyde-3-phosphate dehydrogenase (GAPDH) expression. PCR primer sequences are summarized in Table 2. For analysis of GPCR RNA expression of human chondrocytes, we downloaded the expression data with GEO accession number GSE86578. In GSE86578, RNA from three individual patient samples was stimulated with IL-1 + OSM. Then we performed Student's *t*-test to check which GPCR genes had significantly changed expression between IL-1 + OSM *versus* control.

2.10. Luciferase assay

ATDC5 cells were transfected with pGL3-basic or NF-κB luciferase reporter plasmid using Lipofectamine 2000 for 24 h, then the cells were pre-treated with 5 μM 6-OAU or 50 μM lauric acid for 6 h, following stimulated with 5 ng/mL IL-1β for 12 h. Luciferase assays were performed with Dual luciferase reporter assay kit (Promega, USA).

2.11. Western blotting assay

Whole-cell protein extracts were obtained using Radioimmunoprecipitation assay lysis buffer, separated by 10 % SDS polyacrylamide gel electrophoresis, and transferred to nitrocellulose membranes. After blocking in 5 % BSA, the membranes were incubated with primary an-

Table 2
Primer sequences for RT-qPCR.

Gene Name	Primer sequences
Acan	F: CCCTCGGGCAGAAGAAAGAT R: CGCTTCTGTAGCCTGTGCTTG
Col2a1	F: TTGAGACAGCACGACGTGGAG R: AGCCAGGTTGCCATCGCCATA
Sox9	F: CGGCTCCAGCAAGAACAAG R: GCGCCCACACCATGAAG
Prg4	F: TGGAGTGCTGTCCTGATTTCAAGAG R: GGTGATTTGGGTGAGCGTTTGGTA
Gapdh	F: AGGTCGGTGTGAACGGATTTG R: TGTAGACCATGTAGTTGAGGTCA
Mmp3	F: TTGACTCAAGGGTGGATGCTGTCT R: GCACATGCTGAACAAAGCACTTCC
Mmp13	F: GTGTGGAGTTATGATGATGT R: TGCGATTACTCCAGATACTG
Nos2	F: TCACTGGGACAGCACAGAAT R: TGTGTCTGCAGATGTGCTGA
Adamts5	F: CCCAGGATAAAACCAGGCAG R: CGGCCAAGGGTTGTAAATGG
Gpr84	F: CTCCTGCTACCATGAGTCTGT R: GTGCAGTAGAGTAGATCAGCCA
C5ar1	F: ATGGACCCCATAGATAACAGCA R: GAGTAGATGATAAGGGCTGCAAC
P2ry6	F: GTGAGGATTTCAAGCGACTGC R: TCCCCTCTGGCGTAGTTATAG
S1pr3	F: ACTCTCCGGGAACATTACGAT R: CAAGACGATGAAGCTACAGGTG
Ednra	F: ATGAGTATCTTTTGCCTTGCGG R: GTCTTCCATGTGGCTGCTTAG
Gpr40	F: GCTTTCCATTGAACTTGTTAGCC R: CGCTGAGAGCAGCTAGGAAG
Gpr41	F: CTAAACCTGACCATTTCGGACC R: GATAGGCCACGCTCAGAAAAC
Gpr43	F: TTATTGGCGCTTCGTGTGGAT R: CCTCAGGTAGAACCCCACCA
Gpr120	F: ACCAAGTCAATCGCACCCAC R: GTGAGACGACAAAGATGAGCC
GAPDH	F: CGTCTTCACCACCATGGAGA R: CGGCCATCACGCCACAGTTT
COL2A1	F: CGCCGCTGTCCTTCGGTGTC R: AGGGCTCCGGCTTCCACACAT
ACAN	F: TGGGAACCAGCCTATACCCCAG R: CAGTTGCAGAAGGGCCTTCTGTAC
SOX9	F: GACAGCCCCCTATCGACTTC R: CAAACTCGTTGACATCGAAGG
PRG4	F: CAGAGGTCTCTACTCCAACTACC R: AGTCATTTCAGGTTTAGTCGCTG

*F = Forward Primer, *R = Reverse Primer.

tibody overnight at 4 °C. The membranes were washed three times and incubated with secondary antibodies for 2 h at room temperature. The following antibodies were used: ACAN (Proteintech; 1:500), MMP3 (HuaBio; 1:1000), MMP13 (Servicebio; 1:1000), GAPDH (Cell Signaling Technology; 1:10000), ERK (Cell Signaling Technology; 1:1000), p-ERK (Cell Signaling Technology; 1:1000), JNK (Cell Signaling Technology; 1:1000), p-JNK (Cell Signaling Technology; 1:1000), P38 (Cell Signaling Technology; 1:1000), p-P38 (Cell Signaling Technology; 1:1000), P65 (Cell Signaling Technology; 1:1000), p-P65 (Cell Signaling Technology; 1:1000).

2.12. Statistical analysis

For *in vitro* studies, each experiment was conducted independently three times. Analysis was performed using the SPSS 23.0 statistical software. The data are presented as mean ± S.D. Statistical significance of two independent groups was calculated using two-tailed Student's *t*-test or one-way ANOVA with Dunnett's test used for multiple comparisons test. p values below 0.05 were considered statistically significant.

3. Results

3.1. Gpr84 expression is associated with osteoarthritis

To investigate the role of FFAs in osteoarthritis, IL-1β was used to induce an inflammatory state in chondrocytes [39,40]. We examined the expression of the FFA-sensing GPCRs including *Gpr40*, *Gpr41*, *Gpr43*, *Gpr84*, and *Gpr120* in IL-1β-treated primary cultured mouse articular chondrocytes. Our data showed that *Gpr84* was the only FFA-sensing GPCR upregulated upon IL-1β treatment (Fig. 1A). Moreover, numerous pro-inflammatory mediators including interleukin (IL)-1 and IL-6 family (including IL-6 and oncostatin M (OSM)) perpetuate joint destruction and pathological progression [41–43]. In order to find potential GPCRs associated with human OA pathogenesis, we performed a GEO-genome-wide analysis of all of the GPCRs in human chondrocytes (acc ession file GSE86578) for receptors induced by IL-1 and OSM. Among all of the 826 GPCRs, five GPCR genes (*C5AR1*, GPR84, *S1PR3*, *P2RY6*, *EDNRA*) were upregulated at relatively high levels in human chondrocytes upon IL-1 and OSM stimulation, indicating a potential capacity to regulate OA (Table 3). We then tested *C5ar1*, *S1pr3*, *P2ry6*, and *Ednra* expression in IL-1β-treated primary cultured mouse articular chondrocytes. Interestingly, also only *Gpr84* was upregulated when stimulated with IL-1β (Fig. 1A). This result was confirmed in human chondrocytes (Fig. 1B).

To explore a possible association between GPR84 and OA pathogenesis, we then employed RNAi-mediated knockdown of *Gpr84* in mouse chondrocytes. The downregulation of *Gpr84* markedly promoted the IL-1β-induced expression of matrix-degrading enzymes such as *Mmp3* and *Mmp13* (Fig. 1C-1E). Together, all of these results suggest that *GPR84* is upregulated in IL-1β-induced human and mouse chondrocytes and GPR84 regulates catabolic function in chondrocytes.

3.2. Genetic ablation of Gpr84 aggravates OA pathogenesis in mice

To further investigate the function of Gpr84 in OA pathogenesis, we generated *Gpr84*-knockout (*Gpr84*$^{-/-}$) mice to examined the gene's effect on experimental OA induced by DMM surgery. After 8 weeks of DMM surgery, we performed histological analyses to evaluate the knee joint damage (Fig. 2A). Our data showed that articular cartilage degradation was significantly aggravated in the medial tibial plateau (MTP) and medial femoral condyle (MFC) of *Gpr84*$^{-/-}$ mice (Fig. 2B-2D), and more severe articular cartilage erosion with osteophyte development was observed in *Gpr84*$^{-/-}$ mice (Fig. 2E). Moreover, our micro-CT analysis data showed that abnormal subchondral bone morphology was present in DMM mice, with a higher total subchondral bone tissue volume (TV) and elevated thickness of subchondral bone plate (SBP) in *Gpr84*$^{-/-}$ mice (Fig. 2F-H). Consistent with increased OA, the DMM-induced OA pain was increased in *Gpr84*$^{-/-}$ mice as determined by von Frey tests (Fig. 2I). However, there was no significant difference in synovitis between *Gpr84* knockout mice and WT mice (Fig. 2J and K). Collectively, our results indicate that genetic deletion of *Gpr84* aggravates experimental OA pathogenesis in mice.

To further investigate the effects of *Gpr84*-deficiency on cartilage homeostasis, we examined the expression of chondrocyte homeostasis-

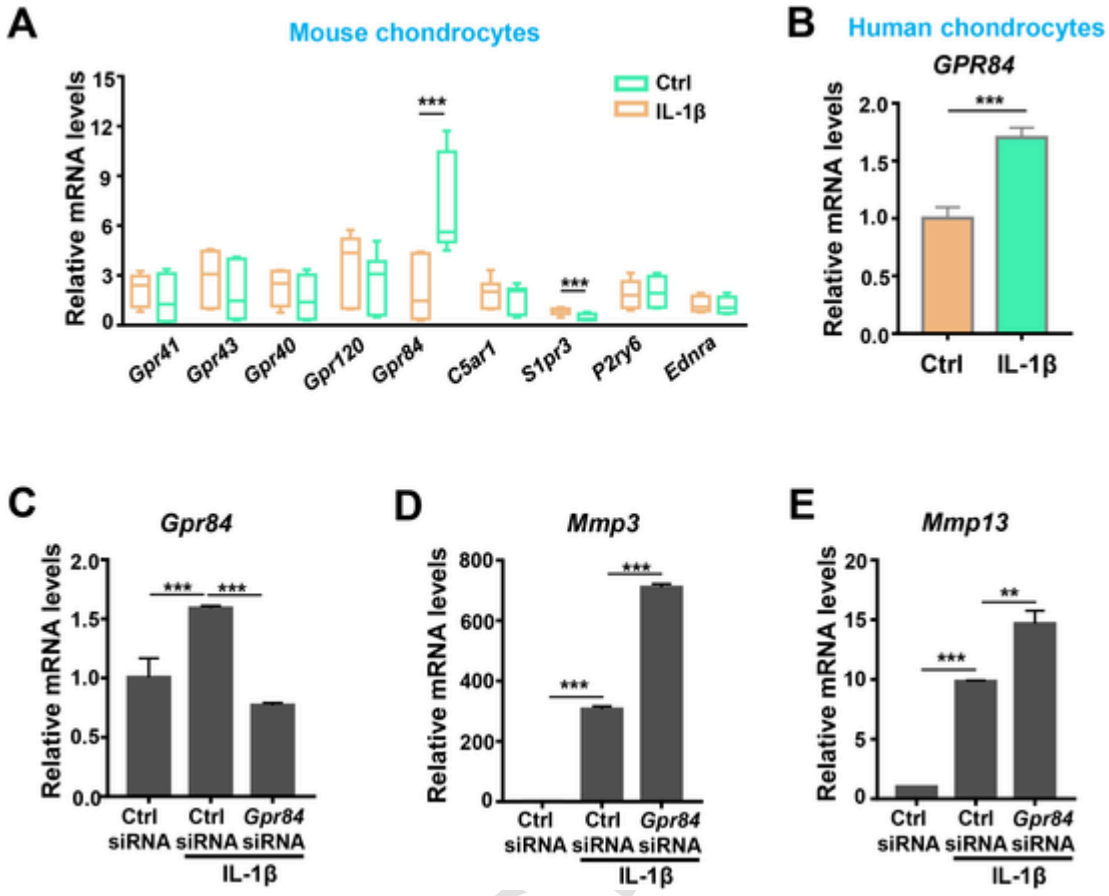

Fig. 1. Expression level of *Gpr84* in IL-1β stimulated chondrocytes and gene expression in chondrocytes with *Gpr84* siRNA.(A) RT-qPCR analysis of mRNA levels of FFA-sensing GPCRs and candidate genes from Table 1 in articular mouse chondrocytes stimulated with 1 ng/mL IL-1β for 24 h. Two-tailed Student's *t*-test was performed with experiments repeated three times independently.(B) *GPR84* mRNA levels as determined by RT-qPCR in human chondrocytes stimulated with 1 ng/mL IL-1β for 24 h. Two-tailed Student's *t*-test was performed with experiments repeated three times independently.(C–E) RT-qPCR analysis of *Gpr84*, *Mmp3* and *Mmp13* mRNA levels in mouse chondrocytes treated with 1 ng/mL IL-1β for 24 h, with or without Gpr84 siRNA. One-way ANOVA followed by Dunnett's test was performed with experiments repeated three times independently. All data were presented as mean ± S.D; * $p < 0.05$, ** $p < 0.01$, *** $p < 0.001$. Experiments repeated three times independently.

Table 3
Gene expression comparing with IL1 + OSM and control articular chondrocytes based on RNA-seq (accession file GSE86578).

Human different expression Genes(GPCRs)	Fold change	P-value
C5AR1	2.04	0.003
GPR84	1.99	0.07
S1PR3	1.94	0.01
P2RY6	1.56	0.001
EDNRA	1.50	0.06

related markers by immuno-histological staining. Our data showed that Mmp13 (a cartilage degradation marker) and Col10a1 (a chondrocyte hypertrophy marker) expression was obviously increased in *Gpr84*$^{-/-}$ mice (Fig. 3A-C). Furthermore, decreased expression of Col2a1 and Aggrecan (Acan), the cartilage anabolic markers, were observed in articular cartilage of *Gpr84*$^{-/-}$ mice (Fig. 3A, D and E). All of the results demonstrated that Gpr84 regulates cartilage homeostasis in both catabolism and anabolism.

3.3. Gpr84 ablation decreases cartilage anabolic factors expression and aggravates IL-1β-induced matrix metalloproteinases expression in vitro

Next, we verified whether Gpr84 regulated IL-1β-induced cartilage catabolic related gene expression, including matrix metalloproteinases (*Mmp3* and *Mmp13*), aggrecanase-1 (*Adamts5*) and nitric oxide synthase-2 (*Nos2*) (Fig. 4A-D). Our results showed that IL-1β-induced expression of *Mmp3* and *Mmp13*, but not *Adamts5* and *Nos2*, were upregulated in *Gpr84*$^{-/-}$ chondrocytes (Fig. 4A-D), which was confirmed by Western blot analysis (Fig. 4G). On the other side, knockout of *Gpr84* decreased the expression of *Acan* and *Col2a1* (the cartilage anabolic genes) by RT-qPCR and reduced Acan expression by Western blot upon IL-1β stimulation (Fig. 4E-G). All of the data demonstrate that Gpr84 has an essential role in regulating both production and degradation of the extracellular matrix during OA pathogenesis.

3.4. Activation of GPR84 suppresses IL-1β-induced NF-κB signaling pathway

IL-1β is implicated in cartilage degradation through regulating NF-κB and MAPKs signaling pathways [44]. To clarify whether Gpr84 modulates the activity of IL-1β signaling, we first analyzed the NF-κB luciferase reporter gene expression stimulated by IL-1β pre-treated with Gpr84 agonists including synthetic compound 6-*n*-octylaminouracil (6-OAU) or natural product lauric acid. Our data showed that 6-OAU or lauric acid could inhibit IL-1β-induced NF-κB activity (Fig. 5A). Consis-

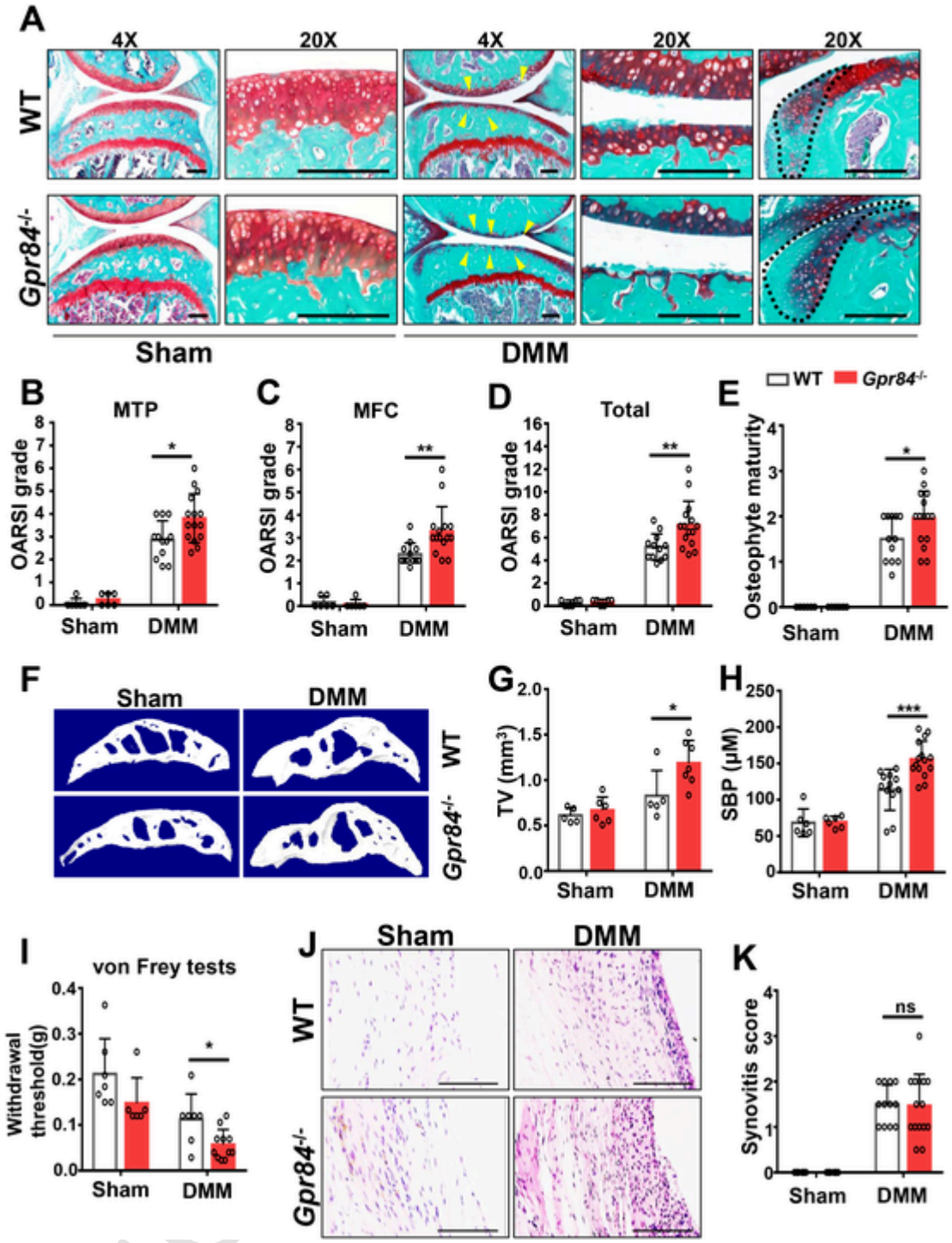

Fig. 2. Genetic ablation of *Gpr84* aggravates OA pathogenesis.After DMM surgery or control (sham) operation for 8 weeks, joints from *Gpr84*$^{-/-}$ mice and WT littermates were isolated and the DMM-induced knee joint damage was assessed.(A) Representative images of safranin O/Fast green staining showing cartilage destruction and osteophyte formation. 20× images: magnified images of articular cartilage and osteophyte. Yellow arrows indicate cartilage destruction, black dotted line indicates osteophyte formation. Scale bar, 200 μm.(B–E) Experimental OA was examined by OARSI scoring, in the medial tibial plateau (MTP) (B), medial femoral condyle (MFC) (C), Total scoring (MTP + MFC) (D) and osteophyte maturity (E). n = 6 for WT and *Gpr84*$^{-/-}$ Sham groups, n = 12 for WT DMM group, n = 15 for *Gpr84*$^{-/-}$ DMM group.(F–H) Subchondral bone morphology. Three dimensional micro-CT images of the tibial subchondral bone medial compartment (sagittal view) of mice in all groups (F), total tissue volume of subchondral bone (TV) (G) and thickness of subchondral bone plate (SBP) (H). Scale bar, 100 μm. n = 5 for WT Sham group, n = 6 for *Gpr84*$^{-/-}$ Sham group, n = 5 for WT DMM group, n = 7 for *Gpr84*$^{-/-}$ DMM group in (G); n = 6 for WT and *Gpr84*$^{-/-}$ Sham groups, n = 12 for WT DMM group, n = 15 for *Gpr84*$^{-/-}$ DMM group in (H).(I) OA-associated pain was measured by the von Frey assays. n = 7 for WT Sham group, n = 6 for *Gpr84*$^{-/-}$ Sham group, n = 7 for WT DMM group, n = 11 for *Gpr84*$^{-/-}$ DMM group.(J and K) Synovial inflammation was determined by H&E staining (J) and analyzed in DMM-operated or sham surgery *Gpr84*$^{-/-}$ mice and WT control (K). n = 6 for WT and *Gpr84*$^{-/-}$ Sham group, n = 12 for WT DMM group, n = 15 for *Gpr84*$^{-/-}$ DMM group. All data were presented as mean ± S.D; * $p < 0.05$, ** $p < 0.01$, *** $p < 0.001$, ns, not significant. Two-tailed Student's *t*-test was performed.

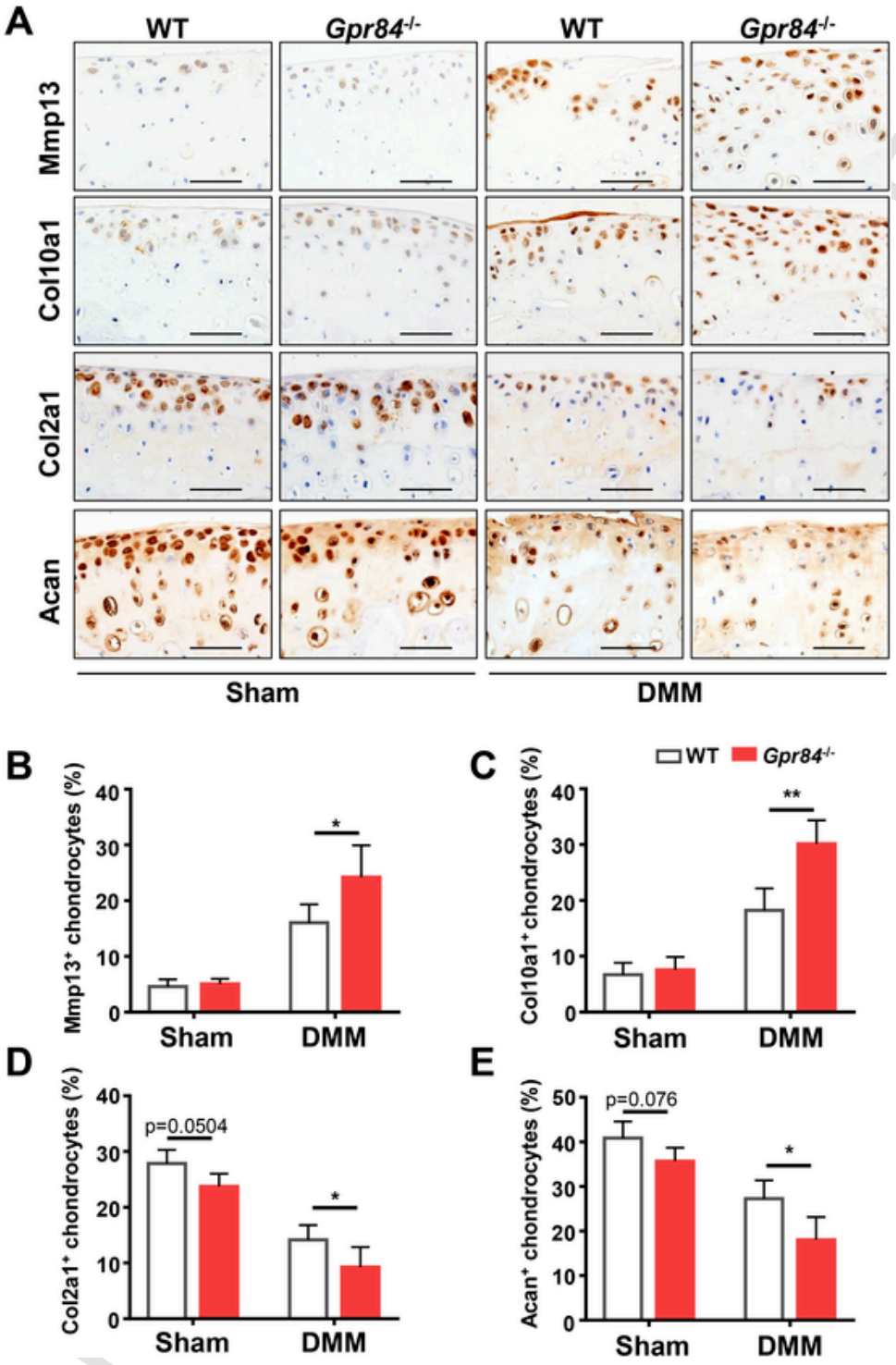

Fig. 3. *Gpr84*-deficiency enhanced cartilage degradation and inhibited ECM generation in OA mouse model.(A) Representative images of immunohistochemistry (IHC) assays of Mmp13, Col10a1, Col2a1 and Acan expression in articular cartilage of mice after DMM surgery or sham control operation for 8 weeks. Scale bar, 50 μm.(B–E) Statistical analysis of the percentage of Mmp13$^+$ (B), Col10a1$^+$ (C), Col2a1$^+$ (D) and Acan$^+$ (E) chondrocytes in articular cartilage of samples shown in A. n = 4; All data were presented as mean ± S.D; * $p < 0.05$, ** $p < 0.01$. Two-tailed Student's *t*-test was performed.

tently, phosphorylation of IκBα and p65 was suppressed by the two GPR84 agonists, especially at 30 and 60 min after IL-1β stimulation (Fig. 5B and C). Furthermore, degradation of IκBα were inhibited in agonist-treated group (Fig. 5B and C). However, the two GPR84 agonists had little effect on the phosphorylation of ERK, JNK, and p38 (Fig. 5B and C). Together, all of the results indicated that Gpr84 attenuates NF-κB signaling.

3.5. Gpr84 regulates cartilage ECM generation

It is known that an imbalance between the anabolism and catabolism of articular cartilage occurs during the development of osteoarthritis. In the pathological progression, the cartilage extracellular matrix is not only degraded, but its synthesis is also inhibited. To evaluate the

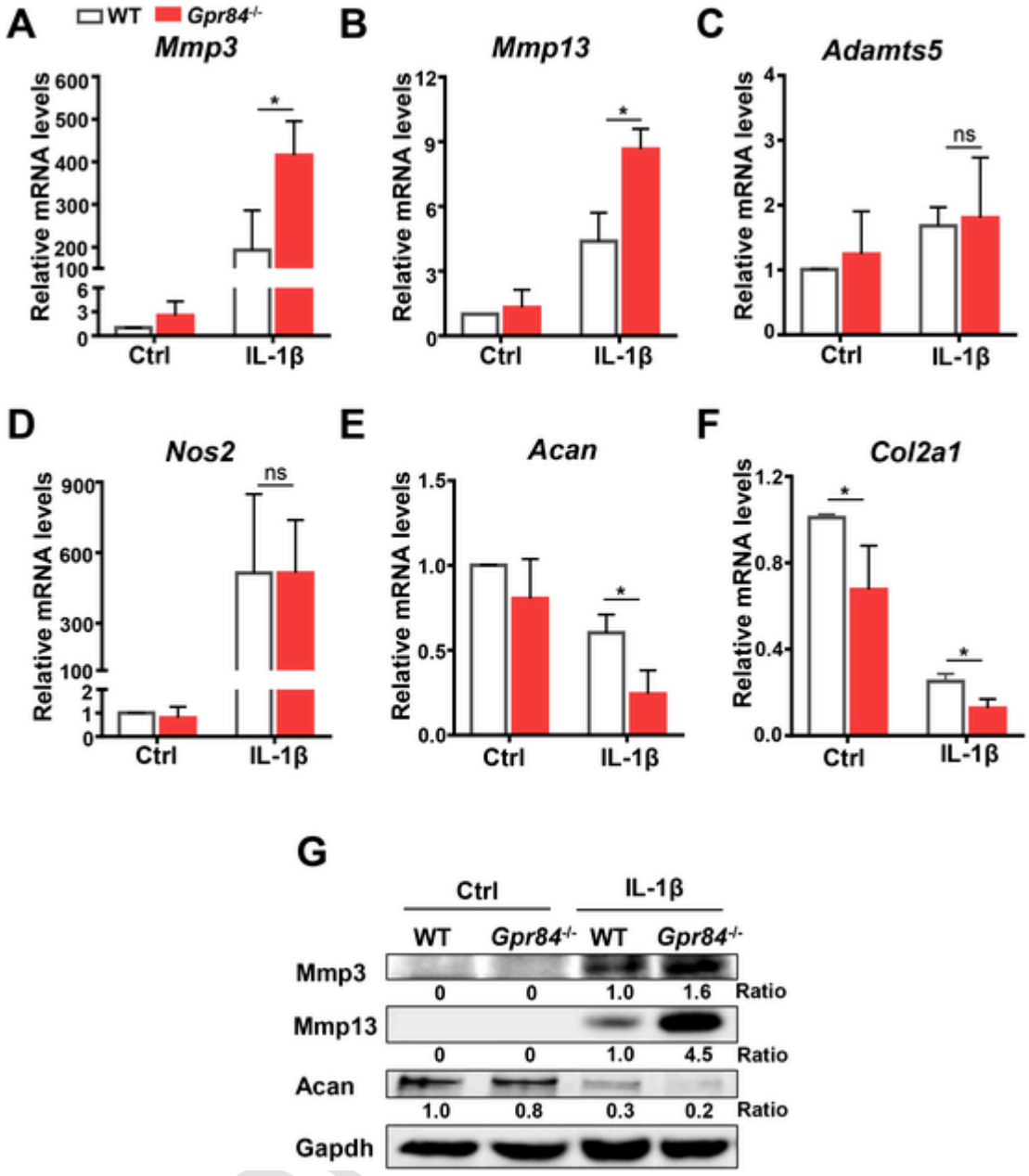

Fig. 4. Knockout of *Gpr84* induces a more severe OA phenotype in mouse articular chondrocytes.(A–F) RT-qPCR analysis of *Mmp3*, *Mmp13*, *Adamts5*, *Nos2*, *Acan* and *Col2a1* mRNA levels in *Gpr84*$^{-/-}$ mice and wild-type control chondrocytes stimulated with IL-1βfor 24 h. All data were presented as mean ± S.D; * $p < 0.05$, ns, not significant.(G) Western blot analysis of Mmp3, Mmp13 and Acan in WT and *Gpr84*$^{-/-}$ chondrocytes treated with 10 ng/mL IL-1β for 36 h.

direct effect of Gpr84 on ECM generation, we employed several approaches. First, we found that the expression of *Gpr84* increased during differentiation of primary mouse articular chondrocytes (Fig. 6A). Next, Alcian Blue staining revealed that *Gpr84*$^{-/-}$ chondrocytes had reduced proteoglycan accumulation during chondrocyte differentiation (Fig. 6B). Moreover, the mRNA expression levels of *Col2a1* and *Acan* were also reduced in *Gpr84*$^{-/-}$ chondrocytes, while proteoglycan 4 (*Prg4*) and SRY-box 9 (*Sox9*) expression has no obvious change (Fig. 6C). Furthermore, the two Gpr84 agonists 6-OAU or lauric acid enhanced the expression of ECM-related genes (*Col2a1* and *Acan*) in mouse articular chondrocytes, but have mild effect on *Prg4* and *Sox9* expression (Fig. 6D). Finally, to investigate whether Gpr84 could modulate ECM generation by stimulating anabolism in human articular cartilage, human OA cartilage explants were cultured in the presence of the two Gpr84 agonists for two weeks. As shown in Fig. 6E, the mRNA levels of *COL2A1* and *ACAN*, but not *PRG4* and *SOX9*, was elevated when treated with 6-OAU or lauric acid compared to the control, indicating that GPR84 could protect human OA cartilage explants against degeneration through inducing cartilage anabolic related gene expression. To evaluate the potential side effects of GPR84 agonists on human chondrocyte, we performed CCK-8 cell viability assay. Our data showed that 6-OAU or lauric acid had little effect on human chondrocyte viability even their concentration is higher than the effective concentration we used (Supplementary Fig. 1). Taken together, these data demonstrated that Gpr84 effectively modulates cartilage ECM generation.

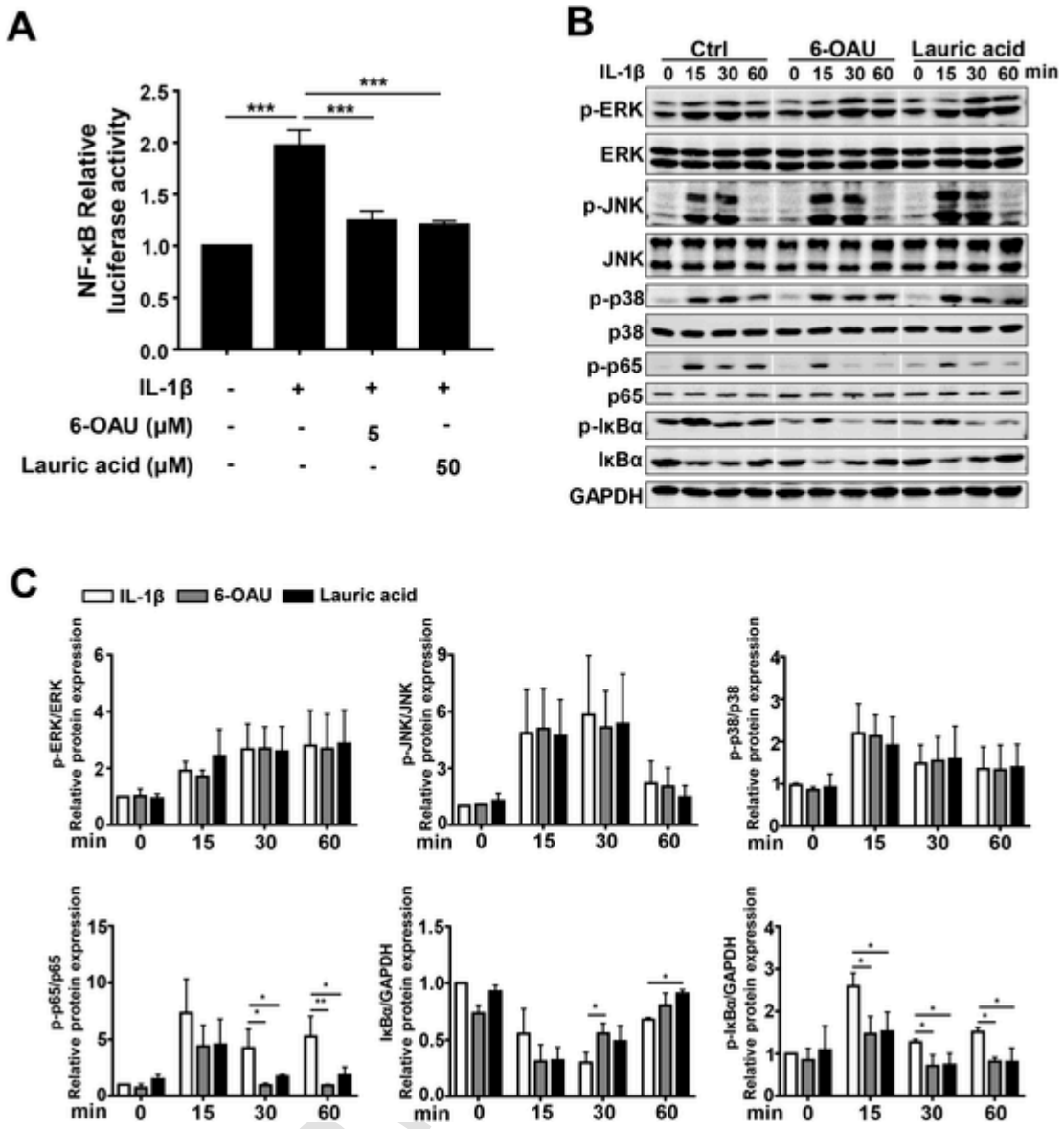

Fig. 5. Activation of Gpr84 inhibits IL-1β-induced NF-κB signaling.(A) Luciferase assay of NF-κB luciferase reporter in ATDC5 cells when treatment with 6-OAU (5 μM) or lauric acid (50 μM) in the presence IL-1β (5 ng/mL) for 12 h. All data were presented as mean ± S.D; *** $p < 0.001$. One-way ANOVA followed by Dunnett's test was performed with experiments repeated three times independently. (B and C) Representative images of Western blot and quantified results of indicated antibodies in ATDC5 cells when treated with IL-1β (10 ng/mL) for the indicated time periods in the presence of 6-OAU (5 μM) or lauric acid (50 μM). The quantified results were shown in (C). One-way ANOVA followed by Dunnett's test was performed with experiments repeated three times independently. * $p < 0.05$, ** $p < 0.01$.

3.6. Gpr84 deletion had little effect on articular and the spine cartilaginous tissues, however, it led to a mild length alteration in the growth plate of long bones

To examine whether Gpr84 regulated the development of cartilage tissue in mice, we investigated the cartilaginous tissues of articular cartilage, the growth plate of the spine and the proximal tibial growth plate in *Gpr84*$^{-/-}$ mice compared with littermate control mice. Our results showed that the thicknesses of total articular cartilage and the ratio of hyaline cartilage to total articular cartilage had no significant difference between the knockout and the wild type mice at 6 weeks and 8 weeks of age (Fig. 7A and B). Similarly, there was no obvious difference in the growth plate and other cartilage tissues of the spine in *Gpr84*$^{-/-}$ mice in 1-, 2-, or 5-month-old mice (Fig. 7C and D).

The length and morphology of the tibial in Postnatal day 1 (P1) and 2-week-old mice showed little differences in proliferating zone (PZ), hypertrophic zones (HZ), growth plate zone (GZ), resting zone (RZ) (Fig. 8A-C). However, a significantly thicker growth plate was observed in *Gpr84*-deficiency mice at 6 weeks and 8 weeks (Fig. 8D-E), including elongated PZ at 6 weeks and HZ at 6 weeks and 8 weeks (Fig. 8D and E). Staining for the hypertrophic chondrocyte marker Col10a1 also confirmed that elongated hypertrophic zones (HZ) were present only in 6- and 8-week-old Gpr84$^{-/-}$ mice, but not in P1 or 2-week-old mice (Fig. 8F and G). Interestingly, postnatal growth plate abnormalities did not affect body length in the *Gpr84*$^{-/-}$ mice (data not show), nor did they affect tibia trabecular bone mass compare to WT controls (Supplementary Fig. 2). Altogether, *Gpr84* deletion had little effect on articular and spine cartilaginous tissues, but had a mild effect on the growth plate length, suggesting that activation of GPR84 has potential in preventing the pathogenesis and progression of OA without severe cartilaginous side effect.

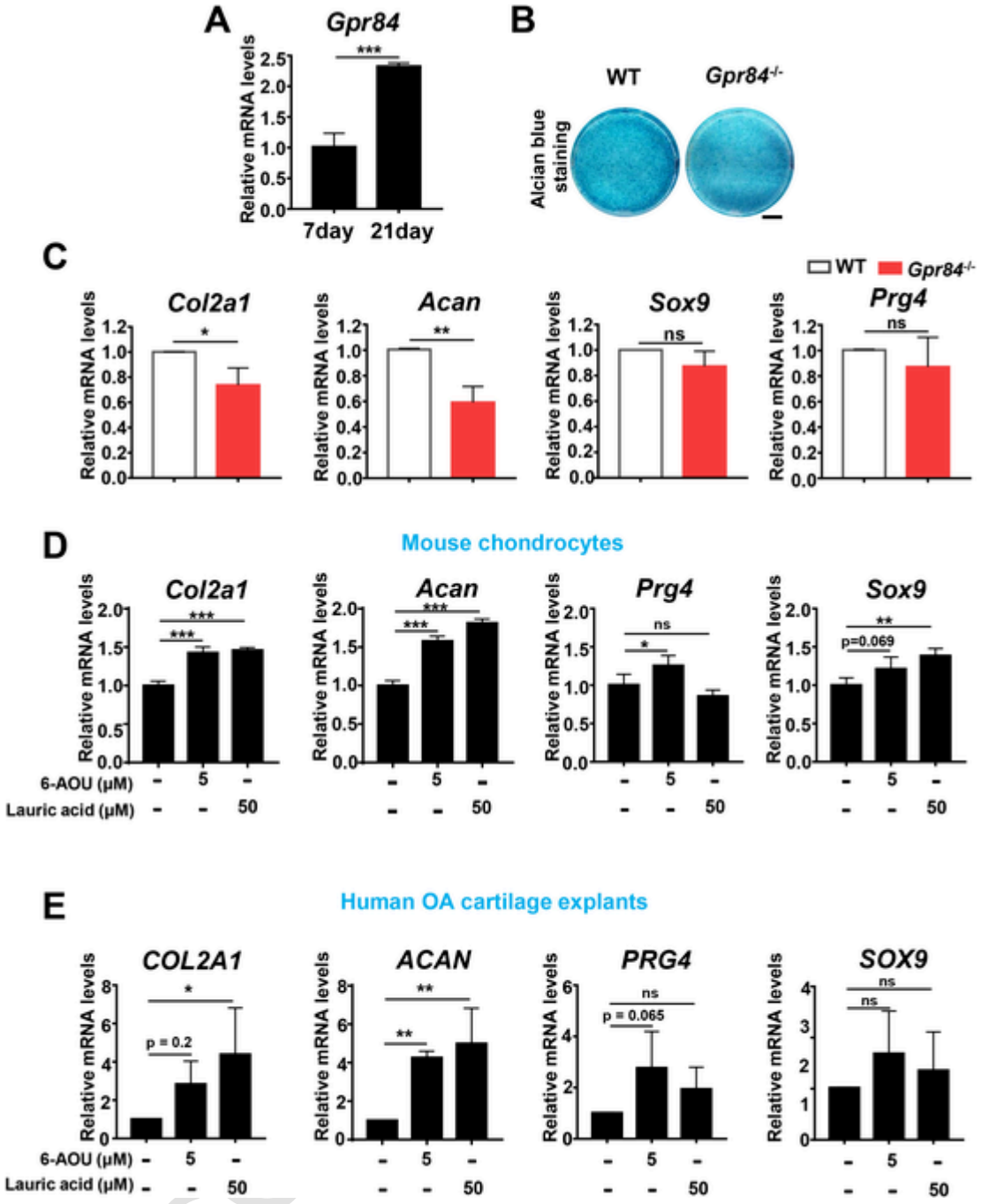

Fig. 6. The effect of *Gpr84* on ECM production.(A) RT-qPCR analysis of *Gpr84* mRNA expression in primary articular chondrocytes at 7 day and 21 day of differentiation. Two-tailed Student's *t*-test was performed with experiments repeated three times independently.(B) Alcian Blue staining showing that *Gpr84*$^{-/-}$ chondrocytes had reduced proteoglycan accumulation compared with WT controls following culture for 14 days in differentiation medium. Scale bar, 5 mm.(C) RT-qPCR analysis *Col2al*, *Acan*, *Sox9* and *Prg4* mRNA levels in *Gpr84*$^{-/-}$ and wild-type control chondrocytes cultured for 14 days in differentiation medium. n = 3; Two-tailed Student's *t*-test was performed.(D) RT-qPCR analysis of *Col2al*, *Acan*, *Sox9* and *Prg4* mRNA levels in chondrocytes cultured for 14 days in differentiation medium with indicated concentrations of the Gpr84 agonist 6-OAU or lauric acid. One-way ANOVA followed by Dunnett's test was performed with experiments repeated three times independently.(E) RT-qPCR analysis of *COL2A1*, *ACAN*, *SOX9*, *PRG4* mRNA levels in human OA cartilage explants after 6-OAU or lauric acid treatment for 2 weeks. n = 3; One-way ANOVA followed by Dunnett's test was performed. All data were presented as mean ± S.D; * $p < 0.05$, ** $p < 0.01$, *** $p < 0.001$, ns, not significant.

4. Discussion

FFA function in cartilage development and OA pathogenesis is poorly investigated. In this study, we found that the FFA-sensing GPCR, Gpr84, was the only FFA-sensing GPCR in mouse and human chondrocytes upregulated by IL-1β. GPR84 was identified as a receptor for MCFAs. *Gpr84*-deficiency increased OA phenotype severity by upregulating catabolic regulators and inhibiting anabolic factors in *Gpr84*$^{-/-}$ mice. Moreover, the agonists of GPR84 protected human OA cartilage explants against degeneration through inducing cartilage anabolic related gene expression. Furthermore, *Gpr84* deletion had little effect on articular and spine cartilaginous tissues during skeletal growth.

Although it's generally known that FFAs have beneficial effects on the skeletal system including bone mass and joint health, only a few studies have examined the effect of MCFAs on the skeletal diseases, particularly on joint health. It has been reported that diets enriched in

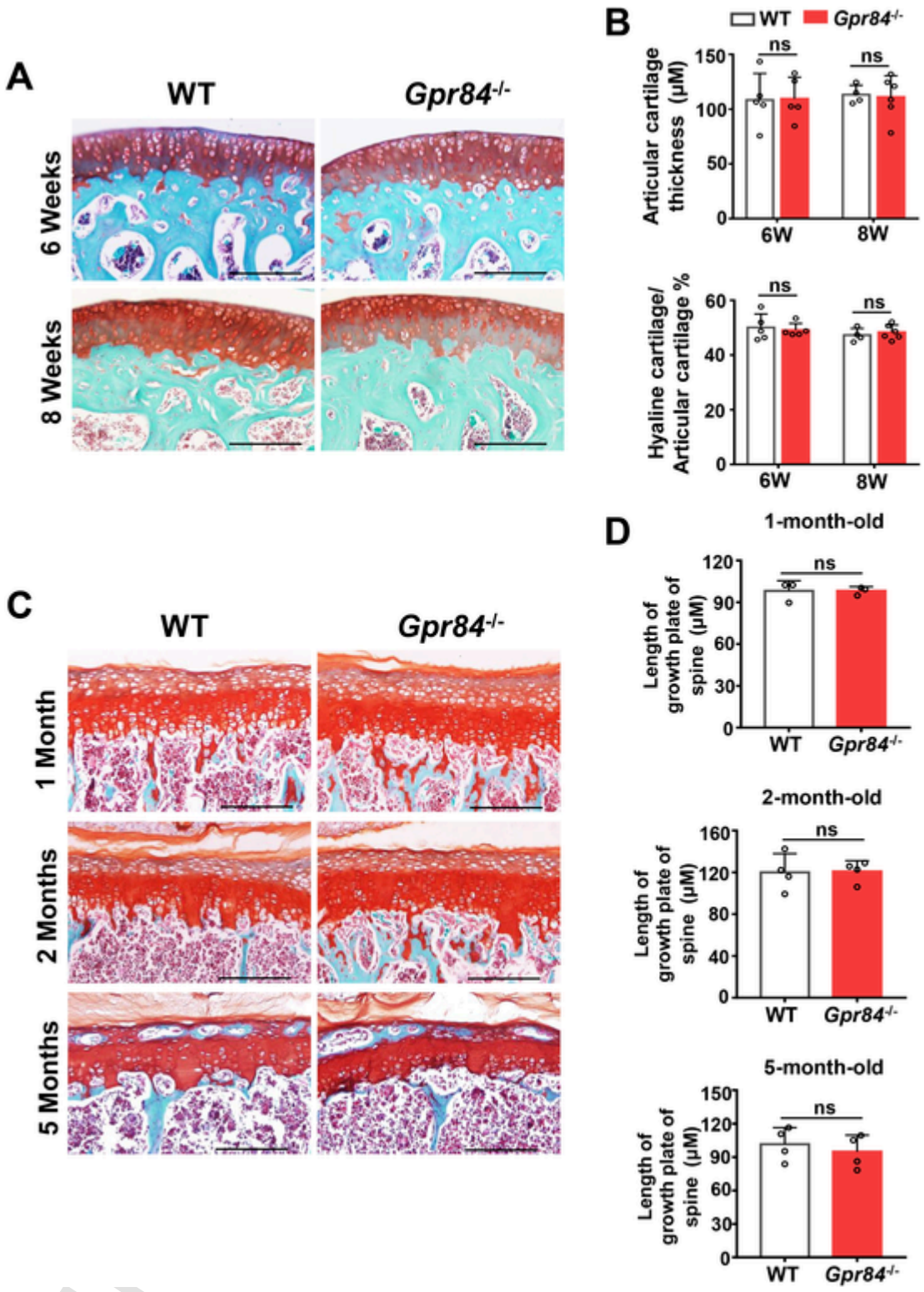

Fig. 7. Genetic ablation of *Gpr84* had little effect on articular and spine cartilaginous tissues during skeletal grow.(A) Histological sections of articular cartilage from 6-week and 8-week-old *Gpr84*$^{-/-}$ and WT mice. Scale bar, 200 μm.(B) The thicknesses of total articular cartilage and the ratio of hyaline cartilage to total articular cartilage articular of samples in (A). All data were presented as mean ± S.D; n = 5 for 6-week-old WT and *Gpr84*$^{-/-}$ groups, n = 4 for 8-week-old WT group and n = 6 for 8-week-old *Gpr84*$^{-/-}$ group; ns, not significant.(C) Histological sections of cartilage tissue of the spine from 1-month, 2-month and 5-month-old *Gpr84*$^{-/-}$ and WT mice. Scale bar, 200 μm.(D) Quantification of the length of the growth plate samples in (C). All data were presented as mean ± S.D; n = 3 for 1-month-old WT and *Gpr84*$^{-/-}$ groups, n = 4 for 2-month and 5-month-old WT and *Gpr84*$^{-/-}$ groups; ns, not significant.

MCFAs lead to lower fat mass and contribute to weight loss in overweight humans [29,45]. Weight loss and reduced body fat mass are effective in the management of OA, as it results in reduced mechanical stress on joints and improved functional capacity, suggesting that MCFA supplementation may have a beneficial role in preventing and treating OA. In the current study, we have shown that deletion of the

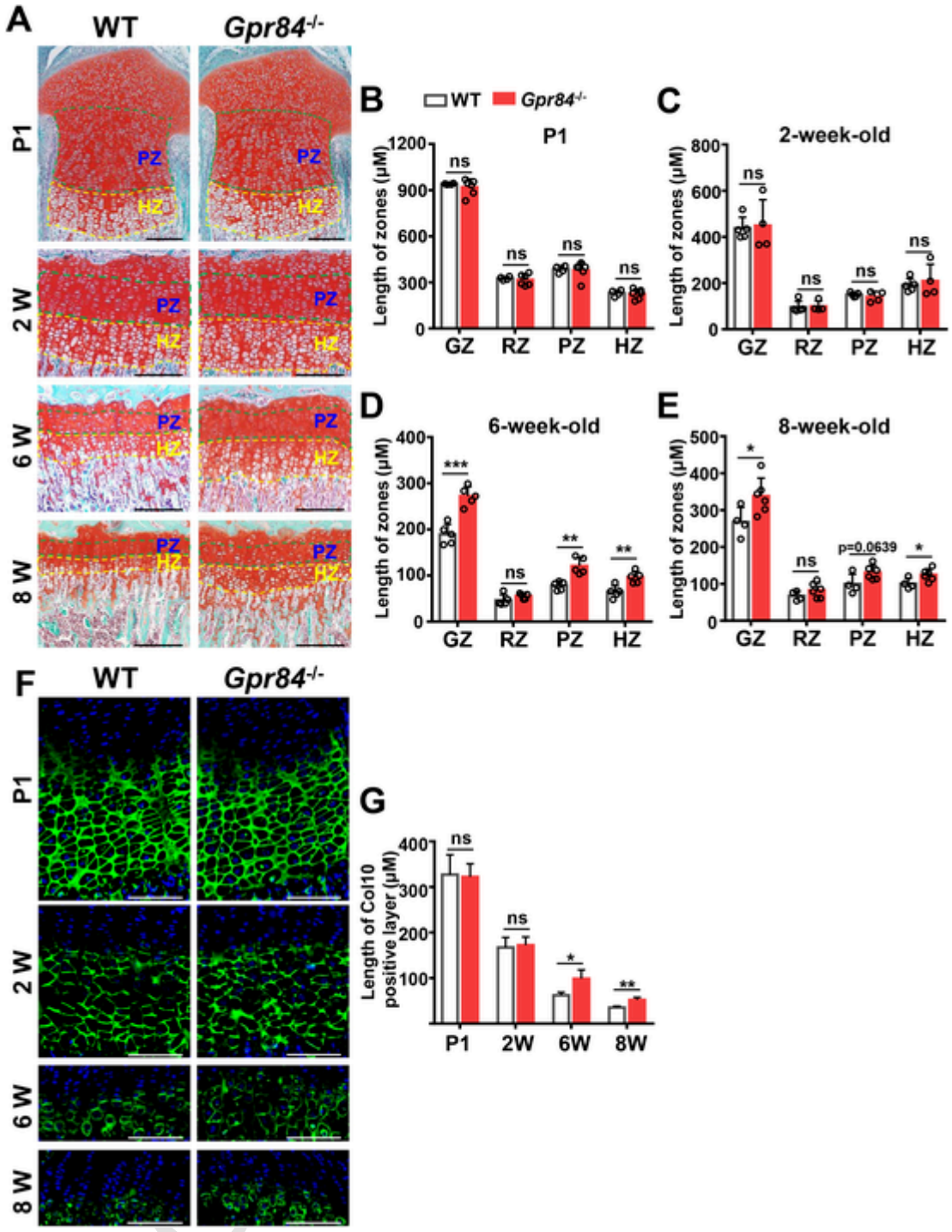

Fig. 8. *Gpr84* deletion led to a mild length alteration in the growth plate of long bones only in 6- and 8-week-old mice.(A) Histological sections of the proximal tibial growth plate from Postnatal day 1 (P1) or 2-, 6- and 8-week-old *Gpr84*$^{-/-}$ and littermate WT mice. PZ, proliferative zone; HZ, hypertrophic zone. Scale bar, 200 μm.(B–E) Quantification of lengths of GZ, RZ, PZ and HZ length in P1 (B), 2-week-old (C), 6-week-old (D) and 8-week-old (E) *Gpr84*$^{-/-}$ and WT mice. GZ, tibia growth plate zone, RZ, resting zone. All data were presented as mean ± S.D; n = 4 for P1-old WT group, n = 6 for P1-old *Gpr84*$^{-/-}$, n = 5 for 2-week-old WT group, n = 4 for 2-week-old *Gpr84*$^{-/-}$group, n = 5 for 6-week-old WT and *Gpr84*$^{-/-}$ groups, n = 4 for 8-week-old WT group and n = 6 for 8-week-old *Gpr84*$^{-/-}$group; * $p < 0.05$, ** $p < 0.01$, *** $p < 0.001$, ns, not significant.(F–G) Immunofluorescence assays of Col10a1 in growth plates from P1, 2-, 6- and 8-week-old *Gpr84*$^{-/-}$ and littermate WT mice (F). Scale bar, 100 μm. Statistical analysis of the length of the Col10a1 positive layer (G). All data were presented as mean ± S.D; n = 4; * $p < 0.05$, ** $p < 0.01$, ns, not significant.

medium-chain FFA receptor, Gpr84, significantly aggravated articular cartilage degradation, osteophyte development and aberrant subchondral bone remodeling. Furthermore, Gpr84 agonists 6-OAU or lauric acid could protect human OA cartilage explants against degeneration through inducing cartilage anabolic related gene expression. All these studies demonstrated a protective role of Gpr84 activation by MCFAs in OA management.

In a diseased state such as OA, disruption of cartilage homeostasis leads to enhanced catabolism and subsequent ECM degradation. In the process, articular chondrocytes lose their differentiated state and enter an endochondral ossification-like process. Chondrocytes undergo hy-

pertrophic differentiation accompanied by expression of Col10a1 and Mmp13, and apoptotic death, which results in mineralization of the cartilage matrix [44,46]. Recently, growing evidence suggests illegitimate hypertrophic differentiation, which contributes to the degradation of cartilage and replacement by bone, plays a critical role in the pathogenesis of OA [47]. Our current study found significantly aggravated articular cartilage degradation and severe articular cartilage erosion with osteophyte development in *Gpr84*$^{-/-}$ mice after DMM surgery. Markers of chondrocyte hypertrophy, such as Col10a1 and Mmp13, were obviously increased in *Gpr84*$^{-/-}$ mice. Interesting, our results showed that *Gpr84* deletion had little effect on articular and spine cartilaginous tissues but had a mild effect on growth plate in long bones only in 6- and 8-week-old *Gpr84*$^{-/-}$ mice. Whereas, the postnatal growth plate abnormalities did not affect body length and trabecular bone mass in the *Gpr84*$^{-/-}$ mice compare to WT controls. It seems that irregular arrangement of the hypertrophic chondrocytes in growth plate has no effect on trabeculae bone formation in physiological conditions. But in pathological conditions as OA, subchondral bone structure of *Gpr84*$^{-/-}$ mice was changed. Whether the activated process of growth plate hypertrophy in *Gpr84*$^{-/-}$ mice can affect the bone remodeling of subchondral bone needs further verification. These results indicated that *Gpr84*-deficiency affected chondrocyte differentiation and hypertrophy under pathological conditions, but very mildly impacted physiological skeletal growth. However, the role of Gpr84 in chondrocyte differentiation and OA should be further validated by cartilage specifically knockout models.

In this study, we performed *in vitro* experiments to indicate that Gpr84 deficiency not only upregulated the expression of matrix-degrading enzymes, but also exerted an inhibitory effect on matrix synthesis. The data showed that activating Gpr84 by 6-OAU or lauric acid resulted in increased expression of ECM-related genes (*Col2a1* and *Acan*) in articular chondrocytes and protected human OA explants against degeneration. In OA pathological progression, disruption of cartilage homeostasis in OA leads to subsequent ECM degradation [48]. Cartilage has rather limited capacities for self-repair and regeneration. Therefore, protection of extracellular matrix from degradation and promoting ECM generation would be an effective therapeutic strategy for OA. Also, ECM regeneration plays a critical role in articular cartilage defects caused by sports-related injury, as cartilage tissue repair remains a significant challenge at present [49,50]. Therefore, the positive effect of Gpr84 on ECM synthesis perhaps provides a promising alternative strategy for treating cartilage defects and osteoarthritis. Furthermore, *Gpr84* deletion had little effect on articular and spine cartilaginous tissues, suggesting that activation of GPR84 has potential in preventing the pathogenesis and progression of OA without severe side effect.

In conclusion, we showed that Gpr84 regulated OA pathogenesis in mice by altering matrix-degrading enzyme expression and ECM synthesis. Moreover, our work suggested that Gpr84 protected human OA cartilage explants against degeneration through inducing cartilage anabolic gene expression. Our results are the first demonstration that Gpr84 played a critical role in OA pathogenesis, and that MCFAs have beneficial effects on joint health.

Author contributions

Study design: F. Wang, Y. Jin, J. Luo; Performed experiments, acquired and interpreted data: F. Wang, L. Ma, Y. Ding, M. Chang, Y. Jin; Reagents, materials and analysis tools: L. Ma, Y. Ding, M. Chang, Y. Shan, L. He, Y. Liu, X. Peng, G. Chen; Manuscript Writing: F. Wang, J. Luo, S Siwko.

Declaration of Competing Interest

The authors declare that there is no conflict of interest.

Acknowledgments

This work was supported by grants from Ministry of Science and Technology of China (2020YFC2002800 to J.L.), the National Natural Science Foundation of China (91949127, 81722020 to J.L., 81974326 to X.P.).

Appendix A. Supplementary data

Supplementary material related to this article can be found, in the online version, at doi:https://doi.org/10.1016/j.phrs.2020.105406.

References

[1] D.J. Hunter, D. Schofield, E. Callander, The individual and socioeconomic impact of osteoarthritis, Nat. Rev. Rheumatol. 10 (7) (2014) 437–441.
[2] Y. Zhang, J.M. Jordan, Epidemiology of osteoarthritis, Clin. Geriatr. Med. 26 (3) (2010) 355–369.
[3] Y.P. Li, Osteoarthritis genetic factors animal models mechanisms and therapies, Front Biosci. E4 (2012) 74–100.
[4] R. Loeser, Osteoarthritis:a disease of the joint as an organ, Arthritis Rheum. 64 (6) (2012) 1697–1707.
[5] S.R. Goldring, Cross-talk between subchondral bone and articular cartilage in osteoarthritis, Arthritis Res. Ther. 14 (2) (2012).
[6] J. Sanchez-Adams, H.A. Leddy, A.L. Mcnulty, The mechanobiology of articular cartilage: bearing the burden of osteoarthritis, Curr. Rheumatol. Rep. 16 (10) (2014) 451.
[7] A. Mobasheri, M.P. Rayman, O. Gualillo, J. Sellam, K. Peter, U. Fearon, The role of metabolism in the pathogenesis of osteoarthritis, Nat. Rev. Rheumatol. 13 (5) (2017) 302–311.
[8] T. Neogi, Y. Zhang, Epidemiology of osteoarthritis, Rheum. Dis. Clin. North Am. 39 (1) (2013) 1–19.
[9] W. Zheng, X. Li, D. Liu, et al., Mechanical loading mitigates osteoarthritis symptoms by regulating endoplasmic reticulum stress and autophagy, FASEB J. 33 (3) (2018) 4077–4088.
[10] D.L. Long, R.F. Loeser, p38γ mitogen-activated protein kinase suppresses chondrocyte production of MMP-13 in response to catabolic stimulation, Osteoarthr. Cartil. 18 (9) (2010) 1203–1210.
[11] S. Rigoglou, A.G. Papavassiliou, The NF- kappa B signalling pathway in osteoarthritis, Int J biochem Cell B. 45 (11) (2013) 2580–2584.
[12] N. Khan, T. Haqqi, Epigenetics in osteoarthritis: potential of HDAC inhibitors as therapeutics, Pharmacol. Res. 128 (2018) 73–79.
[13] N. Koren, S. Simsa-Maziel, R. Shahar, B. Schwartz, E. Monsonego-Ornan, Exposure to omega-3 fatty acids at early age accelerate bone growth and improve bone quality, J. Nutr. Biochem. 25 (6) (2014) 623–633.
[14] L. Knott, N.C. Avery, A.P. Hollander, J.F. Tarlton, Regulation of osteoarthritis by omega-3 (n-3) polyunsaturated fatty acids in a naturally occurring model of disease, Osteoarthr. Cartil. 19 (9) (2020) 1150–1157.
[15] C.L. Wu, D. Jain, J.N. Mcneill, et al., Dietary fatty acid content regulates wound repair and the pathogenesis of osteoarthritis following joint injury, Ann. Rheum. Dis. 74 (11) (2015) 2076–2083.
[16] L. Marieke, J.W. Schoones, M. Kloppenburg, I.F. Andreea, Fatty acids and osteoarthritis: different types, different effects, Joint Bone Spine 86 (4) (2019) 451–458.
[17] C. Montalvany-Antonucci, L. Duffles, J. de Arruda, et al., Short-chain fatty acids and FFAR2 as suppressors of bone resorption, Bone. 125 (2019) 112–121.
[18] S. Lucas, Y. Omata, J. Hofmann, et al., Short-chain fatty acids regulate systemic bone mass and protect from pathological bone loss, Nat. Commun. 9 (1) (2018) 55.
[19] C. Pirozzi, V. Francisco, F.D., et al., Butyrate modulates inflammation in chondrocytes via GPR43 receptor, Cell. Physiol. Biochem. 51 (1) (2018) 228–243.
[20] J. Tan, C. McKenzie, E. Mariño, L. Macia, C. Mackay, Metabolite-sensing g protein-coupled receptors-facilitators of diet-related immune regulation, Annu. Rev. Immunol. 35 (2017) 371–402.
[21] Y. Itoh, Y. Kawamata, M. Harada, M. Kobayashi, M. Fujino, Free fatty acids regulate insulin secretion from pancreatic beta cells through GPR40, Nature. 422 (6928) (2003) 173–176.
[22] C. Tang, K. Ahmed, A. Gille, et al., Loss of FFA2 and FFA3 increases insulin secretion and improves glucose tolerance in type 2 diabetes, Nat. Med. 21 (2) (2015) 173–177.
[23] A. Ichimura, A. Hirasawa, O. Poulain-Godefroy, et al., Dysfunction of lipid sensor GPR120 leads to obesity in both mouse and human, Nature. 483 (7389) (2012) 350–354.
[24] E.D. Toit, L. Browne, H. Irving-Rodgers, et al., Effect of GPR84 deletion on obesity and diabetes development in mice fed long chain or medium chain fatty acid rich diets, Eur. J. Nutr. 57 (5) (2018) 1737–1746.
[25] T. Hara, I. Kimura, D. Inoue, A. Ichimura, A. Hirasawa, Free fatty acid receptors and their role in regulation of energy metabolism, Rev. Physiol. Biochem. Pharmacol. 164 (2013) 77–116.
[26] O. Talukdar, S. Bae, E.J. Imamura, et al., GPR120 is an Omega-3 fatty acid receptor mediating potent anti-inflammatory and insulin-sensitizing effects, Cell. 142 (5) (2010) 687–698.

[27] L.E. Monfoulet, C. Philippe, S. Mercier, V. Coxam, Y. Wittrant, Deficiency of G-protein coupled receptor 40, a lipid-activated receptor, heightens in vitro- and in vivo-induced murine osteoarthritis, Exp. Biol. Med. 240 (7) (2015) 854–866.
[28] Z. Dan, H.K. Wai, L. Sien, et al., GPR120 is an important inflammatory regulator in the development of osteoarthritis, Arthritis Res. Ther. 20 (1) (2018) 163.
[29] M.P. St-Onge, R. Ross, W.D. Parsons, P.J. Jones, Medium-chain triglycerides increase energy expenditure and decrease adiposity in overweight men, Obesity. 11 (3) (2003) 395–402.
[30] M.K. Montgomery, B. Osborne, A.E. Brandon, et al., Regulation of mitochondrial metabolism in murine skeletal muscle by the medium-chain fatty acid receptor Gpr84, FASEB J. 33 (11) (2019) 12264–12276.
[31] M. Suzuki, S. Takaishi, M. Nagasaki, et al., Medium-chain fatty acid-sensing receptor, GPR84, is a proinflammatory receptor, J. Biol. Chem. 288 (15) (2013) 10684–10691.
[32] L.S. Nicol, J.M. Dawes, F.L. Russa, A. Didangelos, S.B. Mcmahon, The role of G-Protein receptor 84 in experimental neuropathic pain, J. Neurosci. 35 (23) (2015) 8959–8969.
[33] M.M. Müller, R. Lehmann, T.E. Klassert, et al., Global analysis of glycoproteins identifies markers of endotoxin tolerant monocytes and GPR84 as a modulator of TNFα expression, Sci. Rep. 7 (1) (2017) 838.
[34] W. Yoon, H.J. Kang, Cho W.Y., et al., G protein-coupled receptor 84 controls osteoclastogenesis through inhibition of NF-κB and MAPK signaling pathways, J. Cell. Physiol. 233 (2) (2018) 1481–1489.
[35] S. Kamekura, K. Hoshi, T. Shimoaka, et al., Osteoarthritis development in novel experimental mouse models induced by knee joint instability, Osteoarthr. Cartil. 13 (7) (2005) 632–641.
[36] V. Krenn, L. Morawietz, G.R. Burmester, R.W. Kinne, T. Haupl, Synovitis score: discrimination between chronic low-grade and high-grade synovitis, Histopathology. 49 (4) (2006) 358–364.
[37] G. Zhen, C. Wen, X. Jia, et al., Inhibition of TGF-β signaling in mesenchymal stem cells of subchondral bone attenuates osteoarthritis, Nat. Med. 19 (6) (2013) 704–712.
[38] R.P. Bonin, C. Bories, Y.A. De Koninck, Simplified up-down method (SUDO) for measuring mechanical nociception in rodents using von Frey filaments, Mol. Pain 10 (1) (2014) 26.
[39] J.H. Kim, J. Jeon, M. Shin, et al., Regulation of the catabolic cascade in osteoarthritis by the zinc-ZIP8-MTF1 axis, Cell. 156 (4) (2014) 730–743.
[40] M. Kapoor, J. Martel-Pelletier, D. Lajeunesse, J.P. Pelletier, H. Fahmi, Role of proinflammatory cytokines in the pathophysiology of osteoarthritis, Nat. Rev. Rheumatol. 7 (1) (2011) 33–42.
[41] M.B. Goldring, Osteoarthritis and cartilage: the role of cytokines, Curr. Rheumol. Rep. 2 (6) (2000) 459–465.
[42] H.E. Barksby, W. Hui, I. Wappler, et al., Interleukin-1 in combination with oncostatin M up-regulates multiple genes in chondrocytes: implications for cartilage destruction and repair, Arthritis Rheum. 54 (2) (2006) 540–550.
[43] M. Nefla, D. Holzinger, F. Berenbaum, C. Jacques, The danger from within: alarmins in arthritis, Nat. Rev. Rheumatol. 12 (11) (2016) 669–683.
[44] T. Saito, A. Fukai, A. Mabuchi, et al., Transcriptional regulation of endochondral ossification by HIF-2α during skeletal growth and osteoarthritis development, Nat. Med. 16 (6) (2010) 678–686.
[45] M.P. St-Onge, A. Bosarge, Weight-loss diet that includes consumption of medium-chain triacylglycerol oil leads to a greater rate of weight and fat mass loss than does olive oil, Am. J. Clin. Nutr. 87 (3) (2008) 621–626.
[46] Y. Hosaka, T. Saito, S. Sugita, T. Hikata, H. Kawaguchi, Notch signaling in chondrocytes modulates endochondral ossification and osteoarthritis development, Proc. Natl. Acad. Sci. U. S. A. 110 (5) (2013) 1875–1880.
[47] Y. Yahara, H. Takemori, M. Okada, et al., Pterosin B prevents chondrocyte hypertrophy and osteoarthritis in mice by inhibiting Sik3, Nat. Commun. 7 (2016) 10959.
[48] K. Yamini, A.J. Grodzinsky, Cartilage diseases, Matrix Biol. 10 (2018) 51–69.
[49] E.B. Hunziker, Articular cartilage repair: basic science and clinical progress. A review of the current status and prospects, Osteoarthr. Cartil. 10 (6) (2002) 432–463.
[50] C. Magali, H. Madry, Biomaterial-guided delivery of gene vectors for targeted articular cartilage repair, Nat. Rev. Rheumatol. 15 (1) (2019) 18–29.